PHYSICAL REVIEW B VOLUME 20, NUMBER 12 15 DECEMBER 1979

Anisotropic contributions to the optical potential employed in theoretical treatments of electron spectroscopies

M. Rasolt and H. L. Davis
Solid State Division, Oak Ridge National Laboratory, Oak Ridge, Tennessee 37830

(Received 9 April 1979)

An analysis is presented which indicates that anisotropic contributions to the optical potential can be caused by the broken symmetry of a surface. This anisotropy is not related to surface plasmons and extends a few layers into the surface region. The anisotropic contributions have been estimated for a simple metal and shown to be of the same order of magnitude as the isotropic contributions. To test possible influences of the anisotropy, a model low-energy electron diffraction (LEED) calculation has been performed. Our results do not show major changes in the LEED I–V profiles, which serve to lend additional credence to previous LEED analyses in which isotropic optical potentials were used. However, it is pointed out that the anisotropic contributions could produce larger effects in other electron spectroscopies (e.g., photoemission).

I. INTRODUCTION

The time evolution of the elastic part of an electron wave function $\phi(\vec{r},t)$ interacting with a scattering system composed of ions and electrons is given by the well-known Dyson equation[1]

$$\left(\frac{-\hbar^2}{2m}\nabla^2 + v(\vec{r})\right)\phi(\vec{r},t) + \int d\vec{r}\,'\,\Sigma(\vec{r},\vec{r}\,',\epsilon_{\vec{p}})\phi(\vec{r}\,',t) = i\hbar\frac{\partial}{\partial t}\,\phi(\vec{r},t)\,, \tag{1}$$

where $v(\vec{r})$ is the ionic potential screened by the electrostatic (or Hartree) potential of the electrons, $\epsilon_{\vec{p}}$ is the energy of the initial wave packet of the interacting electron ($\epsilon_{\vec{p}}$ will be set equal to $\hbar^2p^2/2m$), and Σ is the self-energy. Equation (1) applies for any geometrical configuration of the ions, but in this paper we will restrict our interest only to metallic surfaces. Equation (1) then encompasses in its description, for example, photoemission,[2] Auger electron spectroscopy,[3] low-energy electron diffraction[4] (LEED), and more. A first-principles description of the above processes using Eq. (1), however, is not feasible, owing to the extremely complex structure of the optical potential Σ. This complex structure includes real and imaginary parts which are both nonlocal and energy-dependent,

$$\Sigma(\vec{r},\vec{r}\,',\epsilon_{\vec{p}}) = V_r(\vec{r},\vec{r}\,',\epsilon_{\vec{p}}) + iV_i(\vec{r},\vec{r}\,',\epsilon_{\vec{p}})\,. \tag{2}$$

Our interest here is the structure of the imaginary part, which is second in importance only to the ion-core potential $v(\vec{r})$ in describing the details of the above processes.[4] Although structure can also exist in V_r which could lead to, say, energy shifts of peaks in LEED, any consideration of V_r will be left for future work. We will therefore restrict our attention to the anisotropic contributions to the imaginary part of Σ.

In practice V_i usually has been replaced by a potential which is weakly energy dependent and independent of position.[5] This could be a severe approximation in the surface region, since simple metals have been shown to have significant electronic-density variations normal to the surface.[6] Thus, such an approximation certainly merits close inspection, and, indeed, several aspects have been closely scrutinized. For example, the possibility of a positional dependence arising from core-state polarization has been examined by Ing[7] and shown to be only a small fraction of the conduction-electron contribution. The conduction-electron-density variation in a unit cell, and its effect on V_i, have also been examined by Ing[7] and shown to make less than a 10% contribution for copper. Finally, there is another density variation at the solid-vacuum interface whose effect on V_i was closely examined by Inkson.[8] He finds an additional contribution to V_i from surface plasmons, highly localized at the surface region, within a fraction of an interlayer spacing.

The nonlocal structure of Σ (i.e., its dependence on $\vec{r}$ and $\vec{r}\,'$) introduces additional dependence on the momentum $\vec{p}$ of the scattering electron[9] (see also Sec. II). Because of the broken symmetry along the direction normal to the surface, Σ depends not only on the magnitude $|\vec{p}|$, but also on its direction relative to the normal. Such angular dependence has recently been studied theoretically for photoemission[10] and Auger spectroscopy;[11] these studies were motivated partially by the qualitative observation that surface plasmons become more significant for low grazing angles.[12] In these investigations the metal substrate was replaced by the step model of a surface,[6] and the only intrinsic angular dependence of $V_i(\vec{r},\vec{r}\,',\epsilon_{\vec{p}})$ considered was that due to the emission of surface plasmons when the scattering electron exited from the metal surface.[13]

There is, however, an angular dependence of V_i which is not related to surface plasmons and which is simply a consequence of the broken symmetry along the normal, and extending several layers into the solid. In view of the fact that present theoretical calculations are usually unable to reproduce all details of the data obtained with various electron spectroscopies, we have undertaken a study of these additional contributions to V_i. Our approach is similar to that used in previous theoretical treatment of the isotropic terms. That is, we will first estimate the anisotropic terms theoretically to assess their order of magnitude, and then, realizing that their detailed structure is at present unobtainable, consider them as adjustable parameters in any calculations.

In Sec. II we present a formulation of the additional angular terms. In Sec. III we evaluate these contributions in the random phase approximation (RPA) in the same fashion as has been done for the isotropic calculations.[4] *We find the two terms to be of comparable magnitude.* In Sec. IV we include these terms in a model LEED calculation corresponding to the (100) surface of aluminum. These calculated results are then discussed in Sec. V, where we also suggest possible future work.

II. FORMULATION OF THE ANISOTROPIC CONTRIBUTION TO THE IMAGINARY PART OF THE OPTICAL POTENTIAL

In this section attention is focused on the imaginary part of the self-energy $iV_i(\vec{r},\vec{r}',p_0)$, with $p_0 \equiv \epsilon_{\vec{p}}$, and the approximations we have employed to determine its anisotropic structure are discussed in some detail.

We first note that V_i is a functional of the electronic density $n(\vec{r})$. Sham and Kohn[9] have exploited this property to suggest the following approximation for V_i:

$$iV_i(\vec{r},\vec{r}',p_0) \approx iV_i^h(\vec{r}-\vec{r}',p_0-v(\vec{r}_0),n(\vec{r}_0))\,, \quad (3)$$

where $n(\vec{r}_0)$ is the density at $\vec{r}_0=(\vec{r}+\vec{r}')/2$. The insertion of $v(\vec{r})$ in Eq. (3) is made to maintain the invariance of Eq. (1) under a constant shift of $v(\vec{r})$. Since, however, we will be concerned here with energies p_0 much larger than the nonconstant term of $v(\vec{r}_0)$, this term in Eq. (3) will be neglected. The approximation of Eq. (3) clearly will be the leading term of a gradient expansion for a system of slowly varying density. The hope is that it will remain adequate for actual electronic systems in which the density sometimes varies rather rapidly. To make the solution of Eqs. (1) and (3) more tractable, Sham and Kohn employ yet another approximation and write $\phi(\vec{r},t)$ as a local superposition of plane waves $e^{i\vec{p}(\vec{r})\cdot\vec{r}}$. This is similar in spirit to the WKB approximation and should be quite adequate for the large momentum $\vec{p}(\vec{r})$ of the scattering electron. Then

$$i\int d\vec{r}'\, V_i^h(\vec{r}-\vec{r}',p_0,n(\vec{r}'))\,\phi(\vec{r}',t) = iV_i^h(\vec{p}(\vec{r}),p_0,n(\vec{r}))\,\phi(\vec{r},t)\,. \quad (4)$$

The validity of Eq. (4) depends on the range of the nonlocality $|\vec{r}-\mathrm{r}'|$, the length scale of the density variation $n/\nabla n$, and the wavelength of the momentum $1/p$, which should satisfy $(\nabla n)/pn<1$, as is the case at higher energies. In applications, for example, to LEED calculations,[4] Eq. (4) usually has been simplified even further by averaging over the positional dependence. This yields a single number $iV_i(|\vec{p}|)$ for the imaginary part, which is then considered to be only weakly dependent on the *magnitude* of the scattering electron's momentum. Also, in practice $V_i(|\vec{p}|)$ is usually treated as an adjustable parameter.[5] However, its order of magnitude has been verified for simple metals[4] by calculating the imaginary part of the process given in Fig. 1(b).

It is with the same spirit that we wish to analyze the first higher-gradient corrections to $iV_i(\vec{r},\vec{r}',p_0)$. Equation (3) is now generalized to

$$\begin{aligned} iV_i(\vec{r},\vec{r}',p_0) \approx{}& iV_i^h(\vec{r}-\vec{r}',p_0,n(\vec{r})) + i[\nabla n(\vec{r})\cdot\nabla g_1(\vec{r}-\vec{r}',p_0,n(\vec{r})) + \nabla' n(\vec{r}')\cdot\nabla' g_1(\vec{r}'-\vec{r},p_0,n(\vec{r}))] \\ &+ \tfrac{1}{8} i\{\nabla^2\nabla^2[n(\vec{r})g_2(\vec{r}-\vec{r}',p_0,n(\vec{r}))] + \nabla'^2\nabla'^2[n(\vec{r}')g_2(\vec{r}'-\vec{r},p_0,n(\vec{r}))]\} + O(\nabla n\cdot\nabla n)\,. \end{aligned} \quad (5)$$

There are other terms we can introduce into Eq. (5), but as we shall see shortly, the above form is sufficient and consistent with our order of approximation. We also note that Eq. (5) is constructed so that the operator $iV_i(\vec{r},\vec{r}',p_0)$ is non-Hermitian, and thus probability nonconserving, which is as the absorptive part of the optical potential should be. For a detailed study of the convergence of expansions like Eq. (5), see Ref. 14.

We now follow our initial discussion and operate with iV_i on our WKB wave function and, as for iV_i^h, set the density at $\vec{r}'$ equal to that at $\vec{r}$. Then a bit of algebra yields the following form for the isotropic and anisotropic contributions to the optical potential:

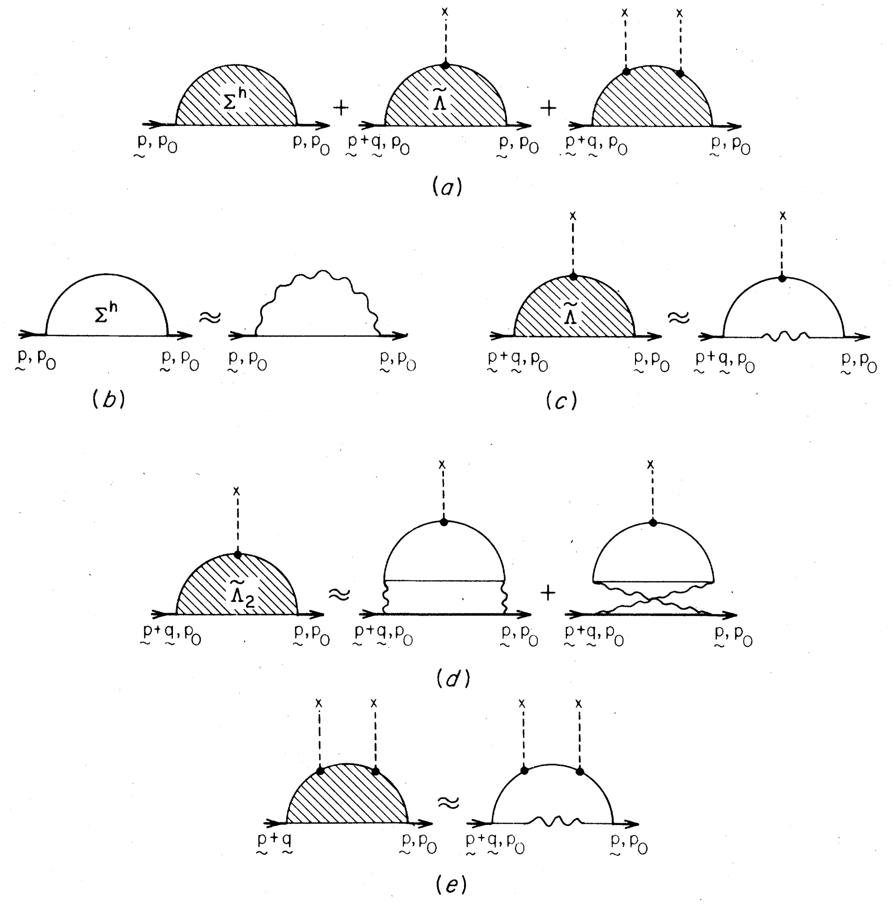

FIG. 1. (a) Contributions to the optical potential to second order in the screened external potential (**×**----); (b) the homogeneous part of the optical potential in the RPA (the wiggly line is the dynamically screened interaction); (c) single-plasmon RPA contribution to the optical potential to linear order in the external potential; (d) two plasmon RPA contributions; (e) example of second-order (in the external potential) contribution to the optical potential in the RPA.

$$i\int d\vec{r}\,'V_i(\vec{r},\vec{r}\,',p_0)\phi(\vec{r}\,',t)=i[V_i^h(\vec{p}(\vec{r}),p_0,n(\vec{r})) -g_2(\vec{p}(\vec{r}),p_0,n(\vec{r}))(\vec{p}\cdot\nabla)(\vec{p}\cdot\nabla)n(\vec{r})+O(\vec{p}\cdot\nabla n\vec{p}\cdot\nabla n)]\phi(\vec{r},t)\,. \tag{6}$$

Of course, a full exposition of all the terms of Eq. (5) in Eq. (6) reveals many additional contributions such as

$$i\,|\vec{p}(\vec{r})|^2\nabla^2 n(\vec{r})\,g_2(\vec{p}(\vec{r}),p_0,n(\vec{r}))\,. \tag{7}$$

However, the terms omitted all depend only on the *magnitude* of the momentum $\vec{p}(\vec{r})$ and therefore will not add any additional angular features to $iV_i^h(\vec{p}(\vec{r}),p_0,n(\vec{r}))$. These terms can be viewed as being part of iV_i^h. To order ∇^2 in the gradient expansion of the optical potential, only the last two terms introduce intrinsic angular dependence in Σ, or equivalently, in iV_i. It is precisely this additional feature that we will investigate in this work.

We conclude this section by making a connection between the anisotropic terms of Eq. (6) and the electron-gas vertex functions. Consider a uniform electron gas to which we introduce an arbitrary external potential $v_{\text{ext}}(\vec{r})$. An example of v_{ext} would be the ionic potential $v(\vec{r})$ in Eq. (1), without the electrostatic screening of the electrons. To second order in v_{ext}, the self-energy Σ is given schematically in Fig. 1(a). The linear term in v_{ext} [Figs. 1(a) and 1(c)] is nothing more than a three-point reducible vertex function[15] $\Lambda(\vec{p}+\vec{q},\vec{p},p_0,n_0)$. The shaded area terminating at the dot is the irreducible vertex function $\tilde{\Lambda}(\vec{p}+\vec{q},\vec{p},p_0,n_0)$, which is related to Λ by

$$\Lambda(\vec{p}+\vec{q},\vec{p},p_0,n_0)=v(\vec{q})[\tilde{\Lambda}(\vec{p}+\vec{q},\vec{p},p_0,n_0)-1]\,, \tag{8}$$

where $v(\vec{q})$ is the Fourier transform of the screened external potential [i.e., $v(\vec{q})=v_{\rm ext}(\vec{q})/\epsilon(\vec{q})$] and is represented by the dashed line in Fig. 1. To first order in $v_{\rm ext}$, V_i is given by

$$iV_i(\vec{r},\vec{r}\,',p_0)\approx iV_i^h(\vec{r}-\vec{r}\,',p_0,n_0)+\left(\int\frac{d^3p}{(2\pi)^3}\,e^{i\vec{p}\cdot(\vec{r}-\vec{r}\,')}\int\frac{d^3q}{(2\pi)^3}\,e^{-i\vec{q}\cdot\vec{r}}\,v(\vec{q})\tilde{\Lambda}(\vec{p}+\vec{q},\vec{p},p_0,n_0)-\text{adjoint}\right). \tag{9}$$

Note that unlike, for example, Eqs. (3) or (4), the density in Eq. (8) is the uniform density n_0, since we are considering V_i, for the moment, strictly to linear order in $v_{\rm ext}$ (see below). Now the density is given in linear response by $n(\vec{q})=-\pi(\vec{q})v(\vec{q})$, where $\pi(\vec{q})$ is the irreducible screening function[16] related to the dielectric function by $\epsilon(\vec{q})=1+(4\pi e^2/q^2)\pi(\vec{q})$. Next we expand $\tilde{\Lambda}$ to second order in q^2, i.e.,

$$\tilde{\Lambda}(\vec{p}+\vec{q}\,,\vec{p},p_0,n_0)\approx-1+\tilde{\Lambda}(\vec{p},\vec{p},p_0,n_0)+\tilde{\Lambda}'(\vec{p},\vec{p},p_0,n_0)\,\vec{p}\cdot\vec{q}+\tilde{\Lambda}_a''(\vec{p},\vec{p},p_0,n_0)(\vec{p}\cdot\vec{q})^2+\tilde{\Lambda}_b''(\vec{p},\vec{p},p_0,n_0)q^2\,. \tag{10}$$

Inserting Eq. (10) in Eq. (9) and replacing $v(\vec{q})$ by $-n(\vec{q})/\pi(\vec{q})$, we obtain for V_i

$$\begin{aligned} iV_i(\vec{r},\vec{r}\,',p_0)\approx{}& iV_i^h(\vec{r}-\vec{r}\,',p_0,n_0)-\int\frac{d^3p}{(2\pi)^3}\,e^{i\vec{p}\cdot(\vec{r}-\vec{r}\,')}\\ &\times\int\frac{d^3q}{(2\pi)^3}\,e^{-i\vec{q}\cdot\vec{r}}\,\frac{n(\vec{q})}{\pi(\vec{q})}\,\{[-1+\tilde{\Lambda}(\vec{p},\vec{p},p_0,n_0)+\tilde{\Lambda}'(\vec{p},\vec{p},p_0,n_0)\vec{p}\cdot\vec{q}\\ &\qquad+\tilde{\Lambda}_a''(\vec{p},\vec{p},p_0,n_0)(\vec{p}\cdot\vec{q})^2+\tilde{\Lambda}_b''(\vec{p},\vec{p},p_0,n_0)q^2]\\ &\qquad-\text{adjoint}\}\,. \end{aligned} \tag{11}$$

If we now set $n(\vec{r})=n_0$ in g_2 of Eq. (6) and perform the integration over $\vec{q}$ in Eq. (10), we can relate g_2 to $\tilde{\Lambda}_a''$ by

$$g_2(\vec{p},p_0,n_0)=-\text{Im}\,\frac{\tilde{\Lambda}_a''(\vec{p},\vec{p},p_0,n_0)}{\pi(0)}\,. \tag{12}$$

It is this function that we approximate in the following section by using the RPA approximation.

The other ∇^2 term in Eq. (6) of order $\nabla n\cdot\nabla n$ can similarly be related to the second order in $v_{\rm ext}$ [Figs. 1(a) and 1(e)]. Since it is a second-order term, however, we expect it to be considerably smaller than the first-order term in Eq. (11). This is particularly true for large momentum of the scattering electron, since the $\nabla n\cdot\nabla n$ term represents a second-order coherent scattering[17] from the external potential in the surface region. For a rapidly moving electron such an event is clearly less likely as the electron traverses this narrow surface region. Mathematically this is reflected through an additional denominator (from an additional electron propagator), entering terms as in Fig. 1(e) as compared to Fig. 1(c). We therefore neglect such contributions in this presentation.

III. EVALUATION OF THE ANISOTROPIC CONTRIBUTION TO THE IMAGINARY PART OF THE OPTICAL POTENTIAL

In this section we evaluate the imaginary part of $\tilde{\Lambda}_a''$ in Eq. (11) within the RPA. Our aim is to estimate its magnitude within the same approximation that has been used formerly for V_i^h.[4]

We could start by applying standard many-body techniques to write the approximate form for the irreducible vertex function $\tilde{\Lambda}$ of the electron gas. However, our concern here is the surface region of a metal, and the long-wavelength fluctuations (or equivalently, the short-wave-vector fluctuations) are poorly represented[18-21] by such homogeneous electron-gas forms, primarily due to contributions from surface plasmons. We therefore choose to start by writing the self-energy Σ within the RPA approximation [Figs. 1(b)][22] for an electron in the presence of the potential $v(\vec{r})$.

The equations that describe this approximation are[1]

$$\Sigma(\vec{r},\vec{r}\,',p_0)=i\int\frac{dk_0}{(2\pi)}\,S_v(\vec{r},\vec{r}\,',p_0+k_0)W(\vec{r},\vec{r}\,',k_0) \tag{13}$$

and

$$W(\vec{r},\vec{r}\,',k_0)=\int d^3r''v_c(\vec{r}-\vec{r}\,'')\epsilon^{-1}(\vec{r}\,'',\vec{r}\,',k_0)\,, \tag{14}$$

where $v_c(\vec{r}-\vec{r}\,')$ is the bare Coulomb interaction and ϵ^{-1} is the inverse of the dynamically screened dielectric function with frequency k_0. S_v is the noninteracting single-particle propagator in the *presence* of $v(\vec{r})$. It satisfies the equation

$$\left[\left(\frac{-\hbar^2}{2m}\nabla^2+p_0\right)+v(\vec{r})\right]S_v(\vec{r},\vec{r}\,',p_0)=-\delta(\vec{r}-\vec{r}\,')\,. \tag{15}$$

We assume that the dielectric function is diagonal in momentum space; that is, we ignore local field corrections.[23-25] Then, in the RPA,

$$\epsilon(\vec{k}, k_0) = 1 + \frac{4\pi e^2}{k^2 V} \sum_{i,j} \frac{|\langle \phi_i | e^{-i\vec{k}\cdot\vec{r}} | \phi_j \rangle|^2}{\hbar k_0 + \epsilon_i - \epsilon_j + i\delta \sin k_0} \times [\theta^<(\epsilon_i - \mu) - \theta^<(\epsilon_j - \mu)], \tag{16}$$

where V is the volume of the electron gas, μ its noninteracting chemical potential $\mu = \hbar^2 k_F^2/2m$, and the ϕ_i satisfy Eq. (15) with the δ function replaced by 0. Also,

$$\begin{aligned} \theta^<(x) &= 0, \quad x > 0 \\ &= 1, \quad x < 0 \\ \theta^>(x) &= 1 - \theta^<(x). \end{aligned}$$

Now Eq. (16) for a surface of a free-electron metal has a rigorous $k \to 0$ limit; it is given by[20-21]

$$\lim_{k\to 0} \epsilon^{-1}(k, k_0) - 1 = \left[V\left(\frac{1}{\epsilon(k_0)} - 1\right) - \frac{A \sin\theta}{k} \times \left(\frac{1}{\epsilon(k_0)} - 1\right) \frac{1 - \epsilon(k_0)}{1 + \epsilon(k_0)} \right]. \tag{17}$$

Here A is the surface area, θ the angle of $\vec{k}$ relative to the surface normal, and $\epsilon(k_0)$ the zero-wave-vector *bulk* dielectric function given by[16]

$$\epsilon(k_0) \equiv \epsilon(0, k_0) = 1 - \frac{\omega_p{}^2}{(k_0 + i\delta)^2}, \tag{18}$$

with δ a positive infinitesimal and ω_p the bulk plasmon frequency, related to the bulk density n_0 by $\omega_p^2 = 4\pi n_0 e^2/m$.

We now employ the following procedures.[20,21] For small wave-vector fluctuations (k small), Eq. (17) is a good approximation for ϵ. Then for for $k < k_c$, where k_c is a cutoff to be chosen below, we approximate ϵ^{-1} in Eq. (14) by Eq. (17). For large wave-vector fluctuations ($k > k_c$), we use the homogeneous-electron-gas result for ϵ^{-1}. The forms for $W(\vec{r}, \vec{r}\,', k_0)$ in the two different regions of k are then inserted in Eq. (13). We will first concentrate on the $k > k_c$ region, which will turn out to be quantitatively most important, and reserve to the end of this section our discussion of the $k < k_c$ contribution to Σ.

Returning to Eq. (13), we first set the screened external potential $v(\vec{r}) = 0$. Then S_v and W reduce to their homogeneous structures, and Eq. (13) yields the bulk form of Σ or iV_i. In other words, $\Sigma \approx \Sigma^h$ or $iV_i \approx iV_i^h$, with fluctuations in the region $k > k_c$. If we add the contribution of the volume term in Eq. (17), we retrieve the full structure of iV_i^h for all k. We next turn on a weak external potential $v(\vec{r})$ and expand both S_v and W to linear order in $v(r)$. The contributions from this expansion to Σ are presented graphically in Figs. 1(c) and 1(d). The wiggly lines are the dynamically screened interactions of the *homogeneous* electron gas with fluctuations restricted to $k > k_c$. The $(\vec{p}\cdot\vec{q})^2$ contribution from the vertex functions of Figs. 1(c) and 1(d) are the appropriate terms for Λ_a'' of Eq. (12). Before we turn to their evaluation let us stress again that these terms could have been automatically written down as the lowest RPA corrections to Σ for a homogeneous electron gas in the presence of a weak external potential. However, due to the presence of a surface, the short-wave-vector fluctuations (surface plasmons) would be poorly treated. The above procedure allows a unified treatment of both regions, and an estimate of the contributions due to surface plasmons will be given at the end of this section. The reader not interested in the key relationships leading to the final form of Eq. (38) may proceed to that equation directly.

Let us next write $\tilde{\Lambda}_1$ for the contribution of Fig. 1(c) and $\tilde{\Lambda}_2$ for the contribution of Fig. 1(d), so that

$$\tilde{\Lambda}(\vec{p}+\vec{q}, \vec{p}, p_0, n_0) = \tilde{\Lambda}_1(\vec{p}+\vec{q}, \vec{p}, p_0, n_0) + \tilde{\Lambda}_2(\vec{p}+\vec{q}, \vec{p}, p_0, n_0). \tag{19}$$

Next expand both $\tilde{\Lambda}_1$ and $\tilde{\Lambda}_2$ to second order in q,

$$\tilde{\Lambda}_1(\vec{p}+\vec{q}, \vec{p}, p_0, n_0) = \tilde{\Lambda}_1(\vec{p}, \vec{p}, p_0, n_0) + \tilde{\Lambda}_1'(\vec{p}, \vec{p}, p_0, n_0)(\vec{p}\cdot\vec{q}) + \tilde{\Lambda}_{1,a}''(\vec{p}, \vec{p}, p_0, n_0)(\vec{p}\cdot\vec{q})^2 + \tilde{\Lambda}_{1,b}''(\vec{p}, \vec{p}, p_0, n_0) q^2 \tag{20}$$

and

$$\tilde{\Lambda}_2(\vec{p}+\vec{q}, \vec{p}, p_0, n_0 = \tilde{\Lambda}_2(\vec{p}, \vec{p}, p_0, n_0) + \tilde{\Lambda}_2'(\vec{p}, \vec{p}, p_0, n_0)\, \vec{p}\cdot\vec{q} + \tilde{\Lambda}_{2,a}''(\vec{p}, \vec{p}, p_0, n_0)(\vec{p}\cdot\vec{q})^2 + \tilde{\Lambda}_{2,b}(\vec{p}, \vec{p}, p_0, n_0) q^2, \tag{21}$$

so $\tilde{\Lambda}_a''$ of Eq. (12) is given by

$$\operatorname{Im} \tilde{\Lambda}_a''(\vec{p}, \vec{p}, p_0, n_0) = \operatorname{Im} \tilde{\Lambda}_{1,a}''(\vec{p}, \vec{p}, p_0, n_0) + \operatorname{Im} \tilde{\Lambda}_{2,a}''(\vec{p}, \vec{p}, p_0, n_0). \tag{22}$$

Following the usual Feynman rules[15] we can write

$$\tilde{\Lambda}_1(p+q, \vec{p}, p_0, n_0) = -\operatorname{tr}_{p', p_0'} \frac{v_c(\vec{p}-\vec{p}\,')}{\epsilon(\vec{p}-\vec{p}\,', p_0 - p_0')} \times S(\vec{p}\,'+\vec{q}, p_0') S(\vec{p}\,', p_0'), \tag{23}$$

where

$$\mathrm{tr}_{p',p_0'}(\cdots)=\int\frac{d^3p'}{(2\pi)^3}\,\frac{dp_0'}{2\pi i}\,(\cdots) \tag{24}$$

and $v_c(\vec{p})=4\pi e^2/p^2$; for notational simplicity we set $\hbar=1$. $S(\vec{p}',p_0')$ is the single-particle propagator of a uniform system,

$$S(\vec{p}',p_0')=\frac{\theta^<(\epsilon_{\vec{p}'}-\mu)}{p_0'-\epsilon_{\vec{p}'}+\mu-i\delta}+\frac{\theta^>(\epsilon_{\vec{p}'}-\mu)}{p_0'-\epsilon_{\vec{p}'}+\mu+i\delta}\,. \tag{25}$$

We next proceed, in some detail, to extract the $(\vec{p}\cdot\vec{q})^2$ contribution in Eq. (23).

We expand $S(\vec{p}'+\vec{q},p_0')$ to order q^2,

$$S(\vec{p}'+\vec{q},p_0')=S(\vec{p}',p_0')+\frac{\partial S}{\partial p_\alpha'}(\vec{p}',p_0')q_\alpha+\frac{1}{2}\,\frac{\partial^2 S(\vec{p}',p_0')q_\alpha q_\beta}{\partial p_\beta'\partial p_\alpha'}+\cdots\,. \tag{26}$$

Here α and β are the three Cartesian coordinates, and repeated indices are summed over. From Eq. (25) the second-order term in Eq. (26) can be written as

$$\frac{1}{2}\,\frac{\partial^2 S}{\partial p_\beta'\partial p_\alpha'}(\vec{p}',p_0')q_\alpha q_\beta=\frac{1}{2m^2}\,\frac{\partial^2 S}{\partial\mu^2}(\vec{p}',\vec{p}')(\vec{p}'\cdot\vec{q})^2-\frac{\partial S}{\partial\mu}(\vec{p}',p_0')\,\frac{q^2}{2m}\,, \tag{27}$$

and the second-order q^2 contribution to $\tilde{\Lambda}_1$ is

$$\tilde{\Lambda}_1=-\mathrm{tr}_{p',p_0'}\left[\frac{v_c(\vec{p}-\vec{p}')}{\epsilon(\vec{p}-\vec{p}',p_0-p_0')}\left(\frac{(\vec{p}'\cdot q)^2}{2m^2}\,\frac{\partial^2 S}{\partial\mu^2}(\vec{p}',p_0')S(\vec{p}',p_0')-\frac{q^2}{2m}\,\frac{\partial S}{\partial\mu}(\vec{p}',p_0')S(\vec{p}',p_0')\right)\right]. \tag{28}$$

The last term in Eq. (28) corresponds to isotropic terms such as those in Eq. (7) and can be neglected. Using the identity

$$\frac{1}{(m-1)!}\left(\frac{-\partial}{\partial\mu}\right)^{m-1}S(\vec{p},p_0)\,\frac{1}{(n-1)!}\left(\frac{-\partial}{\partial\mu}\right)^{n-1}S(\vec{p},p_0)=\frac{1}{(m+n-1)!}\left(\frac{-\partial}{\partial\mu}\right)^{m+n-1}S(\vec{p},p_0) \tag{29}$$

for $m=3$ and $n=1$, and changing variables in the integrals, Eq. (27) can be further simplified to

$$\tilde{\Lambda}_1=\frac{+1}{6m^2}\,\mathrm{tr}_{k,k_0}\left[\frac{v_c(\vec{k})}{\epsilon(k,k_0)}\,((\vec{p}\cdot\vec{q})^2+(\vec{k}\cdot\vec{q})^2+2(\vec{p}\cdot\vec{q})(\vec{k}\cdot\vec{q}))\,\frac{\partial^3 S}{\partial\mu^3}(\vec{p}+\vec{k},p_0+k_0)\right]. \tag{30}$$

There are several ways to evaluate Eq. (30), and we take the most obvious one by explicitly differentiating Eq. (25) with respect to μ to get

$$\begin{aligned}\frac{\partial^3 S}{\partial\mu^3}(\vec{p}+\vec{k},p_0+k_0)={}&-6\pi i\delta'(k_0+p_0-\epsilon_{\vec{p}+\vec{k}})\delta'(\epsilon_{\vec{p}+\vec{k}}-\mu)+2\pi i\delta(k_0+p_0-\epsilon_{\vec{p}+\vec{k}})\delta''(\epsilon_{\vec{p}+\vec{k}}-\mu)\\&+6\pi i\delta''(k_0+p_0-\epsilon_{\vec{p}+\vec{k}})\delta(\epsilon_{\vec{p}+\vec{k}}-\mu)\\&-6\left(\frac{\theta^<(\epsilon_{\vec{p}+\vec{k}}-\mu)}{(p_0+k_0-\epsilon_{\vec{p}+\vec{k}}-i\delta)^4}+\frac{\theta^>(\epsilon_{\vec{p}+\vec{k}}-\mu)}{(p_0+k_0-\epsilon_{\vec{p}+\vec{k}}+i\delta)^4}\right),\end{aligned} \tag{31}$$

where the primes mean derivatives. Consider first the contribution of the last term in Eq. (31) to Eq. (30). With our interest in only the imaginary part of $\tilde{\Lambda}_{1,a}''$ [see Eq. (12)], we evaluate the integral of the last term over k_0 using the well-known analytical structure of $\epsilon(k,k_0)$ to give (for $p>k_F$)

$$\begin{aligned}\mathrm{Im}\,\tilde{\Lambda}_1={}&\frac{1}{48\pi^3m^2}\int_{k_c}^{\infty}k^2dk\,v_c(k)\int d\Omega\;\theta^>(\epsilon_{\vec{p}+\vec{k}}-\mu)\theta^<(\epsilon_{\vec{p}+\vec{k}}-p_0)\\&\times[(\vec{p}\cdot\vec{q})^2+(\vec{k}\cdot\vec{q})^2+2(\vec{p}\cdot\vec{q})(\vec{k}\cdot\vec{q})]\,\mathrm{Im}\left(\frac{\partial^3}{\partial k_0^3}\,\frac{1}{\epsilon(k,k_0)}\right)_{k_0=\epsilon_{\vec{p}+\vec{k}}-p_0},\end{aligned} \tag{32}$$

where Ω is the solid angle. To extract the $(\vec{p}\cdot\vec{q})^2$ term from Eq. (32) we use the identity

$$\cos\theta_{qk}=\cos\theta_{kp}\cos_{qp}+\sin\theta_{qp}\sin\theta_{kp}\cos(\phi_k-\phi_q)\,, \tag{33}$$

where θ_{qk}, θ_{qp}, θ_{pk} are the angles between the vectors $\vec{q}$ and $\vec{k}$, $\vec{q}$ and $\vec{p}$, and $\vec{p}$ and $\vec{k}$, respectively, and ϕ_k ϕ_q are the azimuthal angles of $\vec{k}$ and $\vec{q}$ around $\vec{p}$. We get, after some algebra,

$$\mathrm{Im}\,\tilde{\Lambda}_{1,a}''(\vec{p},\vec{p},p_0,n_0)=\frac{1}{24\pi^2m^2}\int_{k_c}^{\infty}k^2dk\,v_c(k)\int_{-\infty}^{+\infty}dx\;\theta^>(x+1)\theta^>(\epsilon_{\vec{p}+\vec{k}}-\mu)\theta^<(\epsilon_{\vec{p}+\vec{k}}-p_0)\,F(x)\,\mathrm{Im}\left(\frac{\partial^3}{\partial k_0^3}\,\frac{1}{\epsilon(k,k_0)}\right)_{\epsilon_{\vec{p}+\vec{k}}-p_0}, \tag{34}$$

where

$$F(x)=\frac{3}{2}\frac{k^2}{p^2}x^2+\frac{2k}{p}x-\frac{1}{2}\frac{k^2}{p^2}+1 \tag{35}$$

and

$$x\equiv\cos\theta_{kp}\quad\left(\text{since } p_0\equiv\frac{p^2}{2m}\text{ then } \epsilon_{\vec{p}+\vec{k}}-p_0=\frac{k^2}{2m}+\frac{pkx}{m}\right).$$

After a very lengthy analysis, the integral over x in Eq. (34) can be evaluated to give

$$\begin{aligned}\operatorname{Im}\tilde{\Lambda}''_{1,a}(\vec{p},\vec{p},p_0,n_0)=&-\frac{me^2}{6\pi p^4}\int_{k_c}^{\infty}dk\left(\frac{3}{kp}+\frac{2p}{k^3}+\frac{3}{k^2}\right)\theta^{>}\left(\frac{(p-k)^2}{2m}-\frac{k_F{}^2}{2m}\right)\theta^{<}\left(\frac{k^2}{2m}-\frac{pk}{m}\right)\operatorname{Im}\left(\frac{1}{\epsilon(k,y)}\right)\\&+\operatorname{Im}\tilde{\Lambda}''_{1,c}(\vec{p},\vec{p},p_0,n_0),\end{aligned}\tag{36}$$

where $y=k^2/2m-pk/m$. The function $\operatorname{Im}\tilde{\Lambda}''_{1,c}$ in the above equation is

$$\begin{aligned}\operatorname{Im}\tilde{\Lambda}''_{1,c}(\vec{p},\vec{p},p_0,n_0)=&\frac{e^2}{6\pi mp^3}\int_{k_c}^{\infty}dk\left[\frac{(p+3k)(k-p)}{pk^2}\operatorname{Im}\left(\frac{1}{\epsilon(k,y)}\right)+\frac{(k-p)^2}{k}\operatorname{Im}\frac{\partial}{\partial y}\left(\frac{1}{\epsilon(k,y)}\right)\right]\delta\left(y+\frac{p^2}{2m}-\frac{k_F{}^2}{2m}\right)\\&-\frac{e^2}{6\pi}\int_{k_c}^{\infty}dk\,\theta^{>}[k_F^2-(k-p)^2]\left[\frac{3}{kp^5}\operatorname{Im}\left(\frac{1}{\epsilon(k,y_1)}\right)-\frac{1}{mk^2p^2}\right.\\&\qquad\times\operatorname{Im}\left(\frac{\partial}{\partial y_1}\frac{1}{\epsilon(k,y_1)}\right)\frac{dF}{dx}\bigg|_{x=(k_F{}^2-k^2-p^2)/2pk}\\&\qquad\left.+\frac{1}{mpk}\operatorname{Im}\left(\frac{1}{\partial y_1^2}\frac{1}{\epsilon(k,y_1)}\right)F(x)\bigg|_{x=(k_F{}^2-k^2-p^2)/2pk}\right],\end{aligned}\tag{37}$$

where $F(x)$ is given in Eq. (35) and $y_1=k_F^2/2m-p^2/2m$.

To get the final form for $\operatorname{Im}\tilde{\Lambda}''_{1,a}$ from Eq. (30), we must add the contribution from the δ functions in Eq. (31). We will not present the details here, but only state the final results. After a lengthy calculation, these δ functions precisely cancel the term $\operatorname{Im}\tilde{\Lambda}''_{1,c}$ of Eq. (37) and add two additional terms to Eq. (36). The final structure of $\operatorname{Im}\tilde{\Lambda}''_{1,a}$ is now given by

$$\begin{aligned}\operatorname{Im}\Lambda''_{1,a}(\vec{p},\vec{p},p_0,n_0)=&-\frac{e^2m}{6\pi p^4}\int_{k_c}^{\infty}dk\left(\frac{3}{kp}+\frac{2p}{k^3}+\frac{3}{k^2}\right)\theta^{>}\left(\frac{(p-k)^2}{2m}-\frac{k_F^2}{2m}\right)\theta^{<}\left(\frac{k^2}{2m}-\frac{pk}{m}\right)\operatorname{Im}\left(\frac{1}{\epsilon(k,y)}\right)\\&+\frac{e^2}{6\pi p^2}\left[\operatorname{Im}\left(\frac{\partial}{\partial k}\frac{1}{\epsilon(k,y)}\right)_{k=p+k_F}\frac{\theta^{>}(p+k_F-k_c)}{p(p+k_F)}+\operatorname{Im}\left(\frac{\partial}{\partial k}\frac{1}{\epsilon(k,y)}\right)_{k=p-k_F}\frac{\theta^{>}(p-k_F-k_c)}{p(p-k_F)}\right].\end{aligned}\tag{38}$$

where in the last two terms the differentiation is strictly with respect to k after which we set $y=k^2/2m-pk/m$. To obtain the contribution of $g_2(p,p_0,n(\vec{r}))$ [in Eq. (6)] for a varying density $n(\vec{r})$, we evaluate the one-dimensional integral in Eq. (38) for each point $\vec{r}$ by replacing n_0 by its local value $n(\vec{r})$ in $\theta^{>}$ and $\epsilon(k,y)$.

Equation (38) allows for any approximation of the dynamically screened interaction (wiggly line) in Fig. 1(c). In the following section we approximate $\epsilon(k,y)$ by the single-plasmon approximation [Eq. (18)], in which the last two terms of Eq. (38) drop out and the first term can be integrated analytically.

We next turn to $\tilde{\Lambda}_2$, given in Eq. (21) and displayed in Fig. 1(d). Applying again the Feynman rules we obtain

$$\begin{aligned}\tilde{\Lambda}_2(\vec{p}+\vec{q},\vec{p},p_0,n_0)=-2\operatorname{tr}_{p',p_0'}\Bigg\{\operatorname{tr}_{k,k_0}\Bigg[&\left(\frac{v_c(\vec{k}+\vec{q})v_c(\vec{k})}{\epsilon(\vec{k}+\vec{q},k_0)\epsilon(\vec{k},k_0)}S(\vec{p}',p_0)S(\vec{p}-\vec{k},p_0-k_0)\right)\\&\times\left(S(\vec{p}'-\vec{k},p_0'-k_0)S(\vec{p}'+\vec{q},p_0')+S(\vec{p}'+\vec{k},p_0'+k_0)S(\vec{p}'-\vec{q},p_0')\right)\Bigg]\Bigg\}.\end{aligned}\tag{39}$$

Clearly to calculate the $(\vec{p}\cdot\vec{q})^2$ contribution to $\tilde{\Lambda}_2$ is even more difficult than for $\tilde{\Lambda}_1$, and this contribution will not be considered in this presentation. The $\tilde{\Lambda}_2$ terms correspond to coherent[17] absorption and emission of *two* plasmons and are not therefore expected to cancel the $\tilde{\Lambda}_1$ contribution. These terms are not likely to change our estimates and conclusions concerning the *order of magnitude* of the anisotropic terms, which is the purpose of this investigation.

We conclude this section with an approximate treatment of the $k<k_c$ region of $W(\vec{r},\vec{r}',k_0)$. In this region, we use the following forms for W and S_v in Eq. (13):

$$W(\vec{r},\vec{r}',k_0)\approx\int\frac{d\Omega}{(2\pi)^3}\int_0^{k_c}k^2dk\,v_c(k)[\epsilon^{-1}(\vec{k},k_0)-1]e^{i\vec{k}\cdot(\vec{r}-\vec{r}')}, \tag{40}$$

$$S_v(\vec{r},\vec{r}',p_0+k_0)\approx\int\frac{d\Omega}{(2\pi)^3}\int_0^{k_c}k^2dk\,S(\vec{k},p_0+k_0)e^{i\vec{k}\cdot(\vec{r}-\vec{r}')}, \tag{41}$$

with ϵ^{-1} and S defined in Eqs. (17) and (25), respectively.

Applying the WKB approximation (Sec. II) to $\Sigma(\vec{r},\vec{r}',p_0)$, the following form for $V_i(\vec{r},\vec{r}',p_0)$ is readily derived for the $k<k_c$ contribution:

$$\begin{aligned}V_i(\vec{r},\vec{r}',p_0)&\approx V_i(\vec{p},p_0,n_0)\\&=\frac{-A}{V}\frac{1}{4\pi^3}\operatorname{Im}\int d\Omega\int_0^{k_c}\frac{dk}{k}\sin\theta\\&\qquad\times\int dk_0\left(\frac{1}{\epsilon(k_0)}-1\right)\frac{1-\epsilon(k_0)}{1+\epsilon(k_0)}\left(\frac{\theta^<(p^2+k^2+2\vec{p}\cdot\vec{k}-k_F^2)}{k_0-k^2/2m-\vec{p}\cdot\vec{k}/m+k_F^2/2m-i\delta}\right.\\&\qquad\qquad\left.+\frac{\theta^>(p^2+k^2+2\vec{p}\cdot\vec{k}-k_F^2)}{k_0-k^2/2m-\vec{p}\cdot\vec{k}/m+k_F^2/2m+i\delta}\right).\end{aligned} \tag{42}$$

where θ is the angle of $\vec{k}$ relative to the surface normal. It is the $\sin\theta$ in Eq. (42) that makes $V_i(\vec{p},p_0,n_0)$ depend not only on the magnitude of $\vec{p}$ but also on its direction. The contribution from $k<k_c$ that should be included in the anisotropic term of Eq. (6) is the term $(\vec{p}\cdot\hat{z})^2$ in the expansion of Eq. (42) ($\hat{z}\equiv$ a unit vector normal to the surface). Inserting the form of $\epsilon(k_0)$ from Eq. (18), the integral over k_0 in Eq. (42) can be carried out. The $(\vec{p}\cdot\hat{z})^2$ term is then extracted from Eq. (42) by using again the identity in Eq. (33); the result is

$$V_i(\vec{p},p_0,n_0)=\frac{-A}{V}\frac{\omega_p}{8\pi p^3}(\mathrm{p}\cdot\hat{z})^2e^2\left(\int_0^{2\pi}d\phi\,H(k_1,\phi)\theta^>(k_c-k_1)+\int_0^{2\pi}d\phi\,H(k_2,\phi)\theta^>(k_c-k_2)\right), \tag{43}$$

where

$$\begin{aligned}\int_0^{2\pi}d\phi H(k_\alpha,\phi)=\frac{4}{k_\alpha}+\frac{1}{k_\alpha}\int_0^{2\pi}d\phi\Bigg\{&|\sin\phi|\ln\left[\frac{k_\alpha}{k_c}|\sin\phi|+\left(\cos^2\phi+\frac{k_\alpha^2}{k_c^2}\sin^2\phi\right)^{1/2}\right]\\&-\frac{1}{k_c}\left(\cos^2\phi+\frac{k_\alpha^2}{k_c^2}\sin^2\phi\right)^{1/2}\Bigg\}\end{aligned} \tag{44}$$

with $k_1=\omega_p/pk_F$ and $k_2=\omega_p/(\sqrt{2})pk_F$.

In the following section we estimate this contribution from the $k<k_c$ region (or equivalently, from surface plasmons) to the optical potential. The results of Eq. (6), (12), and (38) are then used to perform a model LEED calculation.

IV. NUMERICAL RESULTS AND DISCUSSION

With our main concern the order of magnitude of the anisotropic terms, we will not evaluate the numerical integral over k in Eq. (38). Instead, it is sufficient to approximate $\epsilon(k,y)$ by Eq. (18). The last two terms in Eq. (38) then drop out and the integral can be evaluated analytically to give

$$\begin{aligned}\operatorname{Im}\Lambda''_{1,a}(\vec{p},\vec{p},p_0,n_0)=&\frac{-e^2m^2\omega_p}{12p^4\gamma(p,n_0)}\theta^>\left(\frac{p^2}{2m}-\frac{k_F^2}{2m}-\omega_p\right)\theta^<(k_c-p+\gamma(p,n_0))\\&\times\left[\left(\frac{3}{p[p-\gamma(p,n_0)]}+\frac{3}{[p-\gamma(p,n_0)]^2}+\frac{2p}{[p-\gamma(p,n_0)]^3}\right)\right.\\&\left.-\left(\frac{3}{p[p+\gamma(p,n_0)]}+\frac{3}{[p+\gamma(p,n_0)]^2}+\frac{2p}{[p+\gamma(p,n_0)]^3}\right)\right],\end{aligned} \tag{45}$$

where

$$\gamma(p,n_0)=(p^2-2m\omega_p)^{1/2}\,. \qquad (46)$$

To evaluate the anisotropic term in Eq. (6), we insert the local density $n(\vec{r})$ for n_0 in Eq. (45) and multiply it by $-(\vec{p}\cdot\nabla)(\vec{p}\cdot\nabla)n(\vec{r})$. The cutoff k_c in Eq. (45) is not well known, and many different procedures have been suggested for its evaluation.[18-21] We choose the value suggested in Ref. 20, i.e., $k_c=\beta k_{\mathrm{TF}}$ with $\beta=0.123$, $k_{\mathrm{TF}}=(4k_F/\pi a_0)^{1/2}$ and $a_0=\hbar^2/me^2$. This choice is discussed in detail in Ref. 20. For application to aluminum (a simple metal) we choose for $n(\vec{r})$ the Lang-Kohn[6] density of a step jellium surface with bulk density corresponding to $r_s=2$, where r_s is defined by $(4\pi/3)(r_s a_0)^3=1/n_0$. The anisotropic term is then given by[26]

$$-g_2(\vec{p},p_0,n(\vec{r}))(\vec{p}\cdot\nabla)(\vec{p}\cdot\nabla)n(\vec{r})=\mathrm{Im}\,\Lambda''_{1,a}(\vec{p},\vec{p},p_0,n(z))\,\frac{(\vec{p}\cdot\hat{z})^2}{\pi(0)}\,\frac{\partial^2 n(z)}{\partial z^2}\,, \qquad (47)$$

with $\pi(0)=mk_F/\hbar^2\pi^2$.[27] In Fig. 2 we present the value of Eq. (47) as a function of z and for several energies of the scattering electron. The striking feature of Fig. 2 is that the anisotropic contribution is of the same order of magnitude as the isotropic part. It is about one third the magnitude of V_i^h, which is expected to be about 4 to 6 eV, over a distance of $3.5a_0$ into the bulk. Before we apply this estimate in a model LEED calculation, we turn to an estimate of the surface plasmon contribution [Eq. (44)]. We assume that this contribution occurs when the electron either enters or exits the surface region. The effect on the intensity is then given by dividing Eq. (44) by the current $I=(A/V)(p/m)$, and integrating numerically with the value of k_c given above. We get the change in the intensity of the $(\vec{p}\cdot\hat{z})^2$ term due to the emission of surface plasmons to be of the order of a few percent for $p\simeq 4k_F$.

To investigate possible effects on LEED of anisotropy in the imaginary part of the optical potential, it was decided to perform LEED calculations for a relatively simple model. The motivation for performing such calculations was threefold. First, we wanted to demonstrate that LEED calculations could be performed for a model where anisotropy was included. Second, it appeared desirable to treat a simple case as an initial example in order to minimize the necessary computations. Third, we considered it important to treat a somewhat realistic model so the results might serve to indicate directions for any future work.

Since Al is to a good first-order approximation

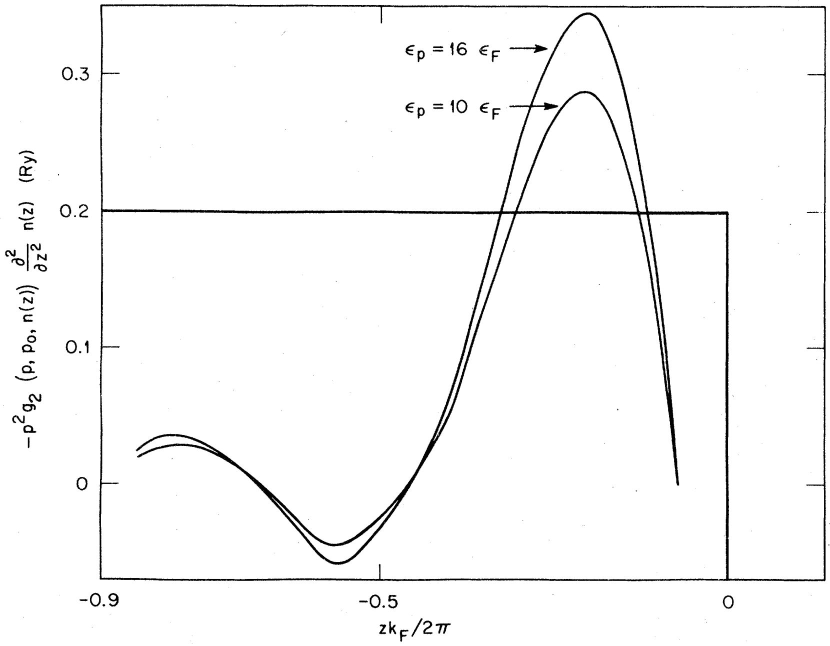

FIG. 2. The anisotropic contribution to the optical potential [Eq. (47)] as a function of position z for two different energies of the scattering electron. The step jellium background is also inserted and the optical potential is terminated by the cutoff k_c [see Eq. (45)] where the long-wavelength fluctuations [Eq. (42)] dominate.

a simple metal to which the analysis of Secs. II and III would be expected to apply, we decided to investigate a model which would correspond to the Al (001) surface. Several previous sets of LEED calculations have been performed for the Al (001) surface.[28-35] Although all these previous calculations were performed using an isotropic V_i, a study of this collected work was quite useful in estimating input parameters for our calculations. For example, we adopted the "no-reflection" boundary-matching procedure of Jepsen *et al.*[32] to match the wave field in vacuum with that in the surface. Also, for the calculations reported here we chose to apply the optical potential at a plane on the vacuum side of the surface at a distance $d/2$ from the atomic centers of the first surface layer. All lattice parameters were set equal to those of the truncated bulk, and d is the perpendicular distance between atomic layers in the surface.

Guided by the analysis of Secs. II and III, the form of the optical potential used in our calculations was

$$\Sigma = V_r + i[\epsilon_2(z) + \epsilon_3(z)\cos^2\theta_p]. \qquad (48)$$

The angle θ_p is between $\vec{p}$ and $\hat{z}$ (the normal to the surface). Since the thrust of the present investigation concerns V_i, V_r was specified to be a constant and equal to -7.5 eV (the value used by Jepsen *et al.*[32]). It is seen from Fig. 2 that the anisotropic part of V_i has its largest deviation from zero in the region of the first layer of the surface; thus, for simplicity in an initial calculation, it was decided to let $\epsilon_3(z)$ be a constant in this region and zero elsewhere. Also, since θ_p is relatively small over the major portion of the energy range of a typically measured LEED I–V profile, it appeared reasonable that the sum of $\epsilon_2(z)$ and $\epsilon_3(z)$ should approximately equal the value used for the isotropic V_i in a previous calculation (e.g., Jepsen *et al.*[32] employed -4.1 eV). For the above reasons, we have performed LEED calculations where $\epsilon_2(z) = -6$ eV and $\epsilon_3(z) = +2$ eV for that part of the surface from $d/4$ on the vacuum side to $d/2$ on the material side of the first atomic layer. Elsewhere in the surface region, the values $\epsilon_2(z) = -4$ eV and $\epsilon_3(z) = 0$ were employed. This model for the Al (001) surface is to be considered only as a simple but somewhat realistic specification which has enabled an initial study to be made concerning possible influences of the anisotropy on LEED I–V profiles.

Existing dynamical LEED computer codes[36,37] have been modified to incorporate the type of anisotropic V_i specified above. These codes are based on the layer KKR formalism and renormalized forward scattering (RFS) perturbation theory for treating the scattering between atomic layers.[32,38] Some typical results obtained from these codes are presented in Fig. 3. The curves of this figure denoted "A" were obtained using the anisotropic V_i described in the preceding paragraph, while those denoted "I" were obtained using an isotropic V_i with $\epsilon_2(z) = -4$ eV and $\epsilon_3(z) = 0$ throughout the entire surface region. The results of Fig. 3 were obtained using Snow's Al band structure potential.[39] Also, 8 phase shifts, 49 beams, 14 atomic layers, and 3 passes of RFS were employed. These Al (001) calculations were performed to correspond to room temperature, and a Debye temperature of 426 K was used to specify isotropic atomic vibrations. The initial beam geometry for the results of Fig. 3 was for an angle of 15° between the bombarding beam and the surface normal, with the azimuth of the incident beam in the plane defined by the reflected (10) and (20) beams. The beams are labeled according to the primitive two-dimensional unit cell as done by, e.g., Tucker and Duke.[40]

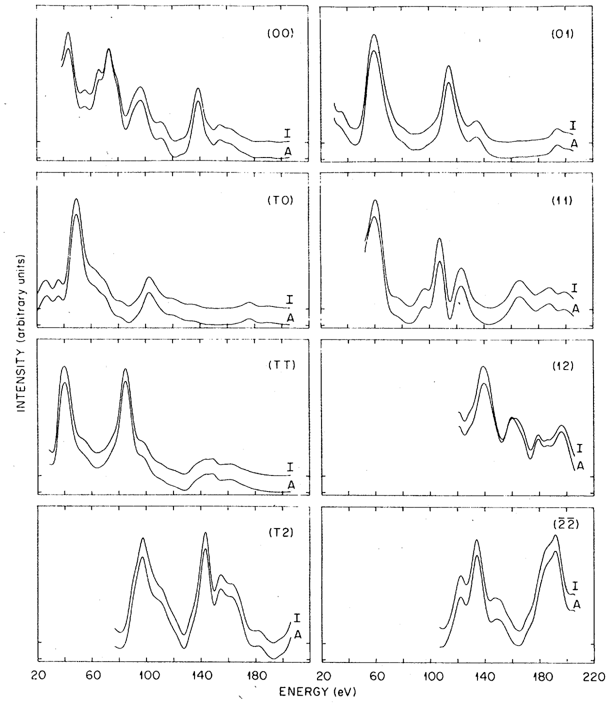

FIG. 3. LEED results for various beams from a model for the Al(001) surface. The curves denoted "I" and "A" were obtained using, respectively, an isotropic and anisotropic imaginary part of the optical potential. Different intensity normalizations have been used for two curves of each subplot in order to have the major peaks be of the same intensity. The dash marks on the vertical axes denote the respective intensity zeros.

V. SUMMARY AND DISCUSSION

An analysis has been presented which shows that anisotropic contributions to the optical potential employed in theoretical treatments of electron spectroscopies can be caused by the broken symmetry of a surface and the resulting variation in the conduction-electron density. These anisotropic contributions have been estimated for a simple metal [i.e., the (001) surface of Al] and shown to be smaller, but of the same order of magnitude, as the isotropic contributions. Because such anisotropic contributions could conceivably affect, say, I–V profiles in LEED, several model LEED calculations were performed to test possible influences of the anisotropy. Some of the results of these calculations are presented in Fig. 3, where they are compared with the results of a calculation which neglected any anisotropic contributions to V_i.

Although it is perhaps surprising considering the model for V_i employed to obtain the anisotropic results, the two curves for each beam of Fig. 3 are seen to be quite similar in their major features. However, it is fortunate that such similarities were obtained, because significant dissimilarities would raise serious questions concerning the very considerable amount of recent LEED work which has inferred surface crystallographic details from I–V profiles (e.g., interlayer spacings of clean surfaces). But some differences between the curves are apparent in Fig. 3; we direct the reader's attention to the 160-eV region in the (12) beam, the differences in relative intensities in the first two major peaks of the (00) beam, and the changes in the shoulders of some of the peaks in the various beams. These differences, however, should not influence crystallographic conclusions in any major way. One reason for the small difference between the curves labeled I and A of Fig. 3 is probably due to the fact that the anisotropic part of V_i is restricted to a narrow region near the surface. On the other hand, it should not be inferred from the results of Fig. 3 that anisotropic contributions to V_i will always be of minor importance. It is possible that LEED results for other surfaces or other geometries would exhibit greater dissimilarities between calculations using isotropic and anisotropic models for V_i. For example, larger differences could occur in LEED calculations for surfaces with fractional overlayers or for reconstructed surfaces because, in both cases, the conduction electron density could vary more rapidly than it does for the Al (001) surface of our example. Only future work can determine the importance of anisotropy in V_i for such cases.

It is also important to consider the influence of anisotropy in V_i for other electron spectroscopies besides LEED. Conceivably the effects of anisotropy in V_i could be more pronounced in the final state (i.e., multiple scattering) effects occurring after electron emission from an atom in the surface region, e.g., photoemission at intermediate energies. We currently expect that the effects would be largest in, say, photoemission as a function of the angle from the surface normal for the case in which the electron emission has occurred in the first or second layer of the surface. Work has been initiated to modify existing computer codes[41] to enable calculations for such a model to be performed.

ACKNOWLEDGMENT

The research for this work was sponsored by the Division of Materials Sciences, U. S. Department of Energy under Contract No. W-7405-eng-26 with the Union Carbide Corporation.

---

[1] L. Hedin and S.Lundquist, in *Solid State Physics*, edited by F. Seitz and D. Turnbull (Academic, New York, 1969), Vol. 23, p. 1.

[2] See, for example, N. V. Smith and W. E. Spicer, Phys. Rev. Lett. 23, 769 (1969); also, Y. Baer and G. Busch, *ibid.* 30, 280 (1973).

[3] See, for example, L. H. Jenkins and M. F. Chung, Surf. Sci. 28, 409 (1971).

[4] J. B. Pendry, *Low Energy Electron Diffraction* (Academic, New York, 1974).

[5] J. E. Demuth, P. M. Marcus, and D. W. Jepsen, Phys. Rev. B 11, 1460 (1975).

[6] See, for example, N. D. Lang and W. Kohn, Phys. Rev. B 1, 4555 (1970).

[7] B. S. Ing, Ph.D. thesis, University of Cambridge, 1972 (unpublished).

[8] J. C. Inkson, Surf. Sci. 28, 69 (1971).

[9] L. J. Sham and W. Kohn, Phys. Rev. B 145, 561 (1966).

[10] M. Sunjic and D. Sokcevic, Solid State Commun. 15, 165 (1974); D. R. Penn, Phys. Rev. Lett. 38, 1429 (1977); R. J. Baird, C. S. Fadley, S. M. Goldberg, P. Z. Feibelman, and M. Sunjic, Surf. Sci. 72, 495 (1978).

[11] P. J. Feibelman, Phys. Rev. B 7, 2305 (1973).

[12] R. J. Baird and C. S. Fadley, results discussed in C. S. Fadley, Prog. Solid State Chem. 11, 265 (1976).

[13] There are obviously extrinsic angular dependences in the scattering amplitude which are kinematic in nature and are related to the length of time an electron spends in the surface region (see Refs. 10 and 11). These, however, are included in a full treatment of the scattering of an electron in the surface region (see Ref. 4).

[14] M. Rasolt, J. S. Y. Wang, and L. M. Kahn, Phys. Rev. B 15, 580 (1977).

[15] P. Noziéres, *Theory of Interacting Fermi Systems* (Benjamin, New York, 1964).

[16] See, for example, D. Pines and P. Nozières, *The Theory of Quantum Liquids* (Benjamin, New York, 1966).

[17] An electron experiences both diffuse and coherent multiple scattering as it passes through the surface region. The former is linear in the coupling and the latter is of higher order.

[18] J. Schmit and A. A. Lucas, Solid State Commun. 11, 415 (1972).

[19] R. A. Craig, Phys. Rev. B 6, 1134 (1972).

[20] V. Peuckert, J. Phys. C 9, 4173 (1976).

[21] D. C. Langreth and J. P. Perdew, Phys. Rev. B 15, 2884 (1977).

[22] Here the propagators and the dynamically screened interaction are those in the presence of the $v(r)$ [i.e., Eqs. (13) and (14)].

[23] S. L. Adler, Phys. Rev. 126, 413 (1962).

[24] J. R. Schrieffer, *Theory of Superconductivity* (Benjamin, New York, 1964), p. 137.

[25] E. O. Kane, Phys. Rev. B 5, 1493 (1972).

[26] In applying Eq. (47) to a calculation of the scattering amplitude a correction from the charge renormalization Z should be included (see Ref. 4). However, for large p and small r_s this correction is relatively small and should not significantly change our estimates for the effect of the anisotropic terms.

[27] See, for example, J. M. Ziman, *Principles of the Theory of Solids* (Cambridge University Press, London, 1964).

[28] S. Y. Tong and T. N. Rhodin, Phys. Rev. Lett. 26, 711 (1971).

[29] D. W. Jepson, P. M. Marcus, and F. Jona, Phys. Rev. Lett. 26, 1365 (1971).

[30] G. E. Laramore and C. B. Duke, Phys. Rev. B 5, 267 (1972).

[31] R. H. Tait, S. Y. Tong, and T. N. Rhodin, Phys. Rev. Lett. 28, 553 (1972).

[32] D. W. Jepsen, P. M. Marcus, and F. Jona, Phys. Rev. B 5, 3933 (1972).

[33] G. E. Laramore, Phys. Rev. B 6, 1097 (1972).

[34] G. E. Laramore, Phys. Rev. B 6, 2950 (1972).

[35] N. Masud, C. G. Kinniburgh, and J. B. Pendry, J. Phys. C 10, 1 (1977).

[36] H. L. Davis, J. R. Noonan, and L. H. Jenkins, Surf. Sci. (to be published).

[37] J. R. Noonan, H. L. Davis, and L.H. Jenkins, J. Vac. Sci. Technol. 15, 619 (1978).

[38] J. B. Pendry, J. Phys. C 4, 3095 (1971).

[39] E. C. Snow, Phys. Rev. 158, 683 (1967).

[40] C. W. Tucker, Jr. and C. B. Duke, Surf. Sci. 24, 31 (1971).

[41] H. L. Davis, p. 2281 in *Proceedings of the 7th International Vacuum Congress and 3rd International Conference on Solid Surfaces* (Vienna, 1977).